

The Analysis of the Actual Surface Structure and Functional Parameters of Materials After Mechanical Processing

P. BORAL*

Czestochowa University of Technology, Faculty Mechanical Engineering, 42-201 Czestochowa, Poland

Doi: [10.12693/APhysPolA.145.762](https://doi.org/10.12693/APhysPolA.145.762)

*e-mail: piotr.boral@pcz.pl

The paper describes the change in the mechanical and microstructural properties of the material after machining with an end mill with variable machining kinematics. The developed model of surface topography was verified after machining with an end mill with a spherical end surface. Also, the author analyzed the correspondence between the experimentally obtained values and the theoretical values obtained using the geometric model. Based on the research presented in the paper, the author demonstrated the influence of the angle of the tool axis arrangement relative to the processed material on changes in the values of surface structure parameters and functional parameters determined on the basis of the material share curve, i.e., the Abbot–Fireston curve for various materials. The tests were performed on the following materials: PA6 aluminum alloy (AW-2017), MO58 free-cutting brass alloy, and NMV tool steel.

topics: milling, surface roughness, machining kinematics

1. Introduction

During the machine cutting, various types of defects can occur, which may have a negative impact on the functional properties of the final product. Research on the formation of the geometric structure of surfaces during machine cutting focuses on the influence of machining parameters on the condition of this surface, typically described by roughness parameters. Regarding surface quality, some studies emphasize the significance of three-dimensional (3D) topography of surfaces, especially in engineering applications [1, 2]. 3D surface topography affects the mechanical and physical properties of contacting parts. It plays a major role in surface integrity, thus influencing fatigue strength. The characterization of surface topography highlights two main issues of equal importance: the definition of appropriate parameters characterizing the three-dimensional surface patterns resulting from multi-axis high-speed machining (HSM) and the evaluation of the relationships between the machining strategy (cutting conditions, machining direction, and tool inclination) with the surface topography.

The geometric structure of the surface formed during milling depends, among others, on tool geometry, machining kinematics, geometric errors of

the elements of the machine tool–holder–workpiece–tool system, displacements caused by forces, vibrations, variability of geometric parameters of the machined layer, blade wear, cutting temperature, stability, etc. Most of the research models developed for analyzing the surface formed during milling do not take into account the combined impact of these factors. Several advanced computer-aided design/manufacturing (CAD/CAM) programs can also be used to prepare surface topography models after milling. Each of these tools offers different functions and capabilities.

There are many publications on the influence of the end milling [3–5] or turning process [6–8] on the development of the mechanical properties of the processed subsurface layers of various materials. Paper [9] presents the optimization of face milling operations for aerospace parts based on finite element method (FEM) simulation and production module (PM) software. In publications [10, 11], the authors studied the impact of machining strategies on the surface quality after milling convex surfaces with a ball-end mill in 3 axes and 5 axes. They showed that the roughness of the free-form surface after milling is significantly influenced by the machining strategy. The researchers [12] discussed the optimization of cutting data and the tool path pattern during the finishing milling of free-form surfaces made of hardened steel.



Fig. 1. Machining of MO58 brass alloy sample.

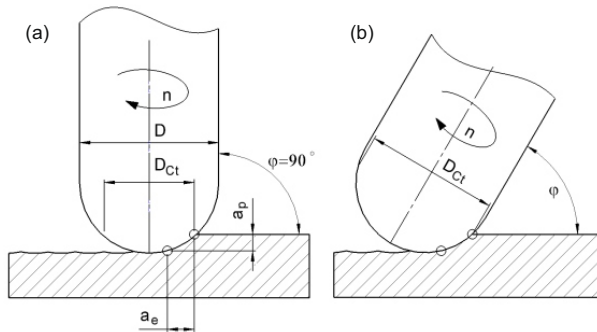


Fig. 2. Tool settings relative to the machined surface: (a) for $\varphi = 90^\circ$, (b) for $\varphi = 45^\circ$.

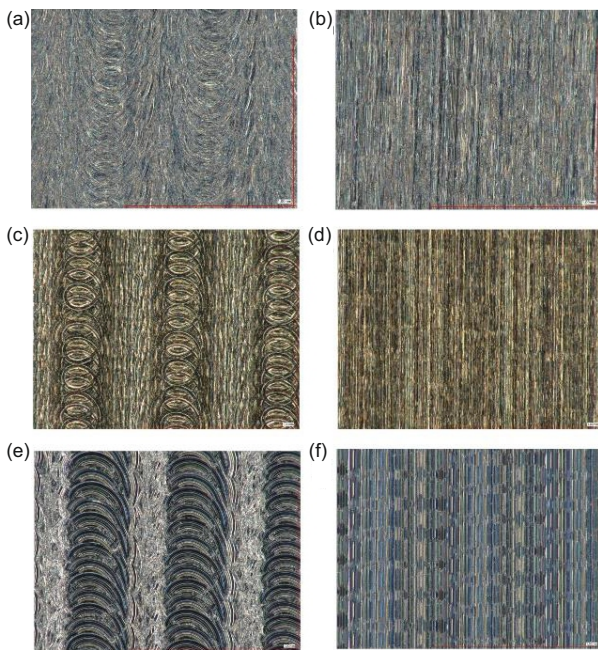


Fig. 3. Surface morphology after milling: at an angle of $\varphi = 90^\circ$ for (a) PA6, (b) MO58, (c) NMV; at an angle $\varphi = 75^\circ$ for (d) PA6, (e) MO58, (f) NMV.

2. Research and results

The machining of samples was carried out with a CMX 50 U series CNC milling machine from DMG MORI with a ball-end mill. A VHM milling cutter with a diameter of $\varnothing 12$ mm from Garant was used for machining samples made of aluminum alloy PA6 (AW-2017) and free-cutting brass alloy MO58 (Fig. 1). However, the machining of the NMV tool steel sample was carried out with a Diabolo VHM HPC ball-end mill with a diameter of $\varnothing 12$ mm from Garant. The following cutting parameters were adopted to prepare the surfaces of samples for testing: depth of cut $a_p = 0.5$ mm, width of cut $a_e = 5\%$ of the cutter diameter (i.e., 0.6 mm), and cutter feed = 0.08 mm/tooth.

This paper presents the results of tests carried out on the mechanical and microstructural properties of the material after machining with an end mill with a ball-end surface.

Changing the angle of the tool axis relative to the machined surface causes a change in the effective diameter of the cutter D_{Ct} (Fig. 2).

In the case of samples made of aluminum alloy and brass alloy, a rotational speed of $n = 10\,000$ rpm was used, and a change in the effective diameter of the cutter D_{Ct} caused a change in the cutting speed in the range of 160–350 m/min. A constant cutting speed of 190 m/min was used for machining tool steel samples. For each material, 10 machining attempts were made, changing the angle of the tool axis relative to the machined surface every 5° , i.e., $90^\circ, 85^\circ, 80^\circ, 75^\circ, 70^\circ, 65^\circ, 60^\circ, 55^\circ, 50^\circ, 45^\circ$. The surface structure analysis was conducted using the Taylor Hobson New Form Talysurf 2D/3D 120 profilometer, equipped with an interferometric transducer head with a resolution of 0.6 nm. The measurements were carried out using a measuring tip in the form of a diamond needle in the shape of a cone ball, with a radius of $2\ \mu\text{m}$ and a cone angle of 90° . TalyMap Platinum 5.1 software from Taylor Hobson was used to analyze the surface topography. After machining in accordance with the established strategy of positioning the tool relative to the sample surfaces and cutting parameters, tests were carried out. Their aim was to determine the influence of the tool axis positioning relative to the machined surface on the quality parameters of the machined surface. It has been observed that during machining at an angle $\varphi = 90^\circ$ (Fig. 3a–c), arc-shaped machining traces appear, which are characteristic of the kinematic–geometric mapping of the cutting edge in the machined material. Nevertheless, in the case when $\varphi < 90^\circ$ (Fig. 3d–f), the surface morphologies do not show visible marks of this type.

The cause of this phenomenon is the relationship between the inclination angle of the machined surface and the effective diameter of the milling cutter, and thus the cutting speed. During machining at $\varphi = 90^\circ$, in the area of the milling cutter's rotation

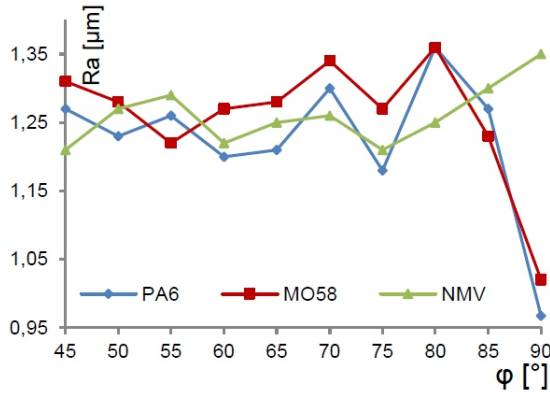


Fig. 4. Surface roughness after milling expressed by the Ra parameter.

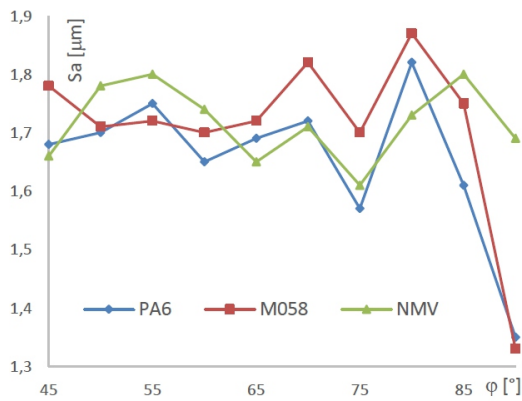


Fig. 5. Surface roughness after milling expressed by the Sa parameter.

axis, the cutting speed v_c is equal to 0 m/min, which contributes to intensify the grooving of the machined material and the formation of plastic flashes on the machined surface. This flash takes the shape of a cutting edge's imprint in the material.

For PA6 samples, it can be observed that the best values of the Sa parameter, which is equivalent to the Ra parameter, are $Sa = 1.35 \mu\text{m}$ and $Sa = 1.57 \mu\text{m}$. These results apply to samples milled at angles of inclination of 90° and 75° , respectively. Therefore, it can be assumed that the best surface roughness parameters were obtained for three inclination angles: 60° , 75° , and 90° . Considering the results of the Ra parameter for brass samples, it was observed that the best values are $Ra = 1.02 \mu\text{m}$, $Ra = 1.22 \mu\text{m}$, $Ra = 1.23 \mu\text{m}$, and $Ra = 1.27 \mu\text{m}$. In this case, the best surface smoothness was achieved for surfaces machined at a 90° angle. Analyzing the surface topography of the NMV tool steel samples, the best surface, based on the evaluation of roughness profile parameters, was found for surfaces machined at angles of 45° and 75° . The value of Ra in this case was $Ra = 1.21 \mu\text{m}$. In all three cases, the best roughness parameters were obtained at a tool angle of 75° , and for samples made of aluminum alloy

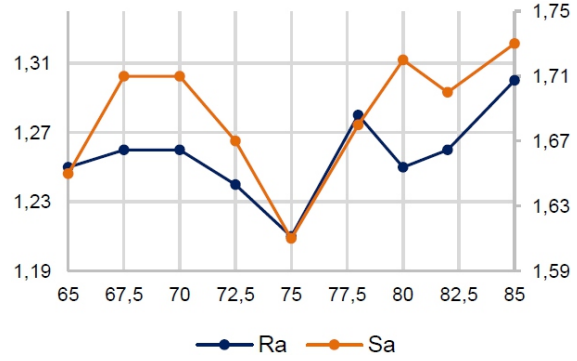


Fig. 6. Surface roughness after milling expressed by Ra and Sa parameters.

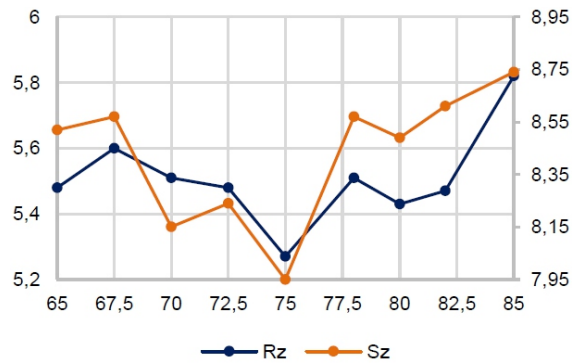


Fig. 7. Surface roughness after milling expressed by Ra and Sz parameters.

and brass alloy, additionally 90° (Figs. 4 and 5). Materials such as PA6 and MO58 are characterized by low hardness and lower tensile strength. Despite the challenging cutting conditions with the tool axis perpendicular to the machined surface, the quality parameters remain good. Based on the presented preliminary analysis, supplementary tests were carried out on the machining of the hardened material (NMV tool steel) in order to obtain the best roughness for the cutting parameters adopted during the main tests. The research was supplemented with subsequent machining trials at the following angles of the tool axis relative to the machined surface: 82.5° , 77.5° , 72.5° , 67.5° .

Based solely on the geometric model derived from the tool geometry, its position relative to the machined surface, and the machining kinematics, without considering all other factors occurring during the milling process, the height of surface irregularities is $\approx 7 \mu\text{m}$. Considering the best values of the Sz parameter, which is equivalent to the Rz parameter, it is $Sz = 7.95 \mu\text{m}$, which was obtained at a tool angle of 75° (Figs. 6, 7). The value of the obtained parameter is comparable to the geometric model.

Taking into account the functional parameters related to the volume, calculated on the basis of the material share (Fig. 8a), the Abbott-Fireston curve or bearing area curve (BAC) shows for a

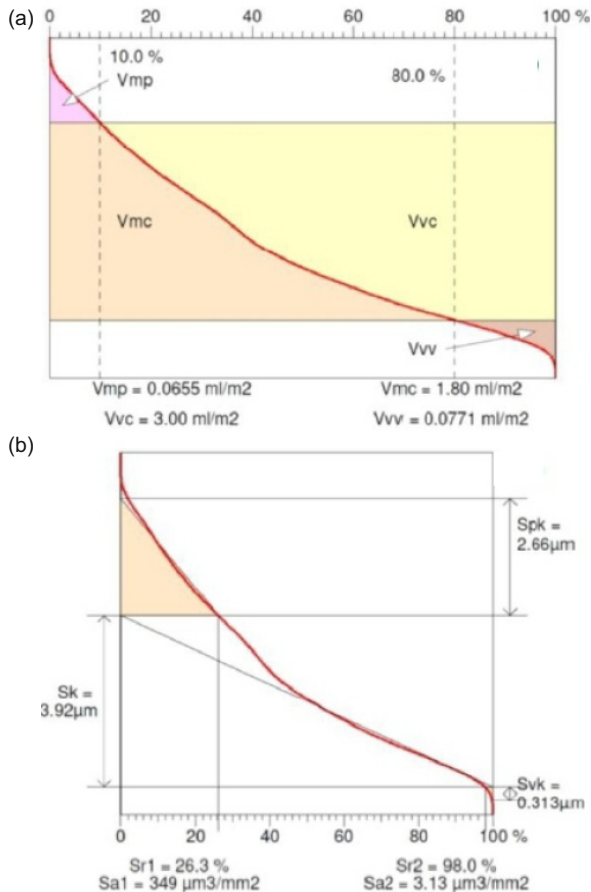


Fig. 8. Abbott–Firestone curve (bearing area curve) for NMV steel samples at an angle of $\varphi = 75^\circ$: (a) surface volumetric functional parameters, (b) position of the linearizing line of the curve, surface amplitude parameters.

specific depth (vertical axis of the graph) the percentage of the cut material in relation to the coated material. The following parameters were obtained: the peak volume of the surface material V_{mp} equal to 0.0655 ml/m^2 , the core volume of the surface material V_{mc} equal to 1.8 ml/m^2 , the volume of the hollow core surface space V_{vc} equal to 3.0 ml/m^2 , and the cavity volume of surface V_{vv} equal to 0.0771 ml/m^2 .

The parameter V_{mp} determines the compliance of the surface during sliding and rolling lapping. In this case, the value of this parameter indicates abrasion resistance, i.e., good running-in behavior. In contrast, the void volume of a recess in the surface V_{vv} is a measure of the oil-holding capacity of the surface.

The tribological properties of the surface can also be assessed by analyzing the bearing area curve (Fig. 8b). The core roughness S_k is $3.92 \mu\text{m}$ and represents the roughness height after initial lapping. The parameters Sr_2 of the material share at the point where the core zone passes into the pits zone

and Sv_k of the reduced valley depth allow for the assessment of the lubricating properties of the surfaces and are a measure of the ability to hold the fluid by the sliding surfaces. In this case, the Sv_k value is relatively small and amounts to $0.313 \mu\text{m}$.

3. Conclusions

Tilting the axis of a ball-end milling tool while cutting material at a shallow depth and width causes the tool to cut outside the axis of the cutter's rotation. This appears to be advantageous due to the kinematic nature of the process itself. The shape and directionality of machining marks during the finish cutting of hardened steel with a ball-end mill are closely dependent on the tilt angle of the machined surface. In the case of hard materials, based on the example of NMV tool steel, the best surface quality parameters were obtained at a tool angle of 75° . For materials with lower hardness and good machinability, the best surface quality after milling with a ball-end mill was achieved with the cutter axis positioned perpendicular to the machined surface.

References

- [1] P. Pawlus, R. Reizer, M. Wieczorowski, *Materials* **14**(18), 5326 (2021).
- [2] P. Boral, R. Gołębcki, *Materials* **15**(18), 6412 (2022).
- [3] M. Storchak, L. Hlembotska, O. Melnyk, *Materials* **17**(7), 1552 (2024).
- [4] Z. Grešová, P. Ižol, M. Vrabež, L. Kaščák, J. Brindza, M. Demko, *Appl. Sci.* **12**(9), 4421 (2022).
- [5] M. Sadílek, Z. Poruba, L. Čepová, M. Šajgalík, *Materials* **14**(1), 25 (2021).
- [6] L. Luo, J. Pang, Y. Song, S. Liu, G. Yin, H. Peng, Ch. Pu, Y. Lin, J. Li, X. Shi, *Arch. Metall. Mater.* **68**(4), 1525 (2023).
- [7] S. Harun, Y. Burhanuddin, G.A. Ibrahim, *J. Manuf. Mater. Process.* **6**(5), 105 (2022).
- [8] D. Xu, L. Ding, Y. Liu, J. Zhou, Z. Liao, *J. Manuf. Mater. Process.* **5**(3), 100 (2021).
- [9] P. Niesłony, W. Grzesik, K. Jarosz, P. Laskowski, *Procedia CIRP* **77**, 570 (2018).
- [10] A.F. de Souza, A. Machado, S.F. Beckert, A.E. Diniz, *Procedia CIRP* **14**, 188 (2014).
- [11] M. Sadílek, L. Kousal, N. Náprstková, T. Sztokowski, J. Hajnyš, *Manuf. Tech. Jour.* **18**(6), 1015 (2018).
- [12] A. Matras, W. Zębala, *Materials* **13**(5), 1109 (2020).